

# ANALYTICAL SOLUTION AND NUMERICAL MODELING OF SLOSHING UNDER RANDOM EXCITATIONS

XIN JIN<sup>1</sup>, PENGZHI LIN<sup>2</sup>

<sup>1</sup>State Key Laboratory of Hydraulics and Mountain River Engineering, Sichuan University, China, bzjx1988@126.com

<sup>2</sup>State Key Laboratory of Hydraulics and Mountain River Engineering, Sichuan University, China, cvelinpz@126.com

## Abstract

Sloshing under random excitations can take place under many circumstances, e.g., liquid sloshing in liquefied natural gas (LNG) tanks during sea and land transportation, water sloshing in large reservoirs during earthquakes, ship motion induced sloshing, and fuel sloshing in aerospace vehicles, and etc. In this study, the two-dimensional sloshing under random surge excitations is investigated analytically and numerically. With the linear wave theory (Faltinsen, 1978), the analytical solution of sloshing under surge excitations with arbitrary phases is obtained. A special wave spectrum and real sea wave data are adopted to generate random sea oscillations. The analytical solution for random excitations is also obtained. The sloshing under random excitations is also studied numerically. With a two-phase fluid model, by solving the spatially averaged Navier-Stokes equations constructed on a non-inertial reference frame, the sloshing is obtained. The analytical solutions are first validated against the numerical results for liquid sloshing with harmonic excitations for inviscid fluids. When the external frequency is close to the fundamental frequency, large discrepancies are developed between the numerical results and the analytical solutions, and this is mainly due to the nonlinearity becomes non-negligible. The analytical solution for the real sea excitation is also compared with the numerical results, and good consistency with the numerical result is guaranteed.

**Keywords:** *Sloshing; random excitation; analytic solution; numerical model; linear wave theory.*

## 1 INTRODUCTION

Liquid sloshing is a classical natural phenomenon, and has caused many attentions. In reality, systems, such as transportation of oil and liquefied natural gas, liquid fuel tanks and etc are always under external excitations. Many researchers are focused on the extreme case, namely resonance, which may cause violent oscillations and large loads on the tank walls when the external excitations are near the natural frequency. More details can be found in a literature review (Ibrahim, 2001).

In the past decades, researchers are mainly devoted to theoretical and numerical study, and experiment is also an effective supplement to investigate sloshing. For analytical research, the potential theory is a powerful tool. In the early years, small amplitude motion was studied systematically (Abramson, 1966). Based on the potential theory, by solving a particularly initial boundary value problem, an analytical solution considering forced surge excitations in a 2-D tank for non-breaking wave was obtained (Faltinsen, 1978), and an artificial damping term was first introduced to model the viscous effect. These theories are validated in the frame of linear theory which assumes that wave amplitudes are generally small, that is, nonlinear hydrodynamic effects are negligible. When the nonlinear effects dominate the sloshing response especially for resonance, the linear theory may be invalid. By considering the linearized free surface conditions and linearized Navier–Stokes equations, an analytical solution considering the nonlinear theory in 2-D rectangular tanks was established (Wu et al., 1998). Some nonlinear analytical solutions were also proposed in literatures (e.g., Faltinsen, 1974; Faltinsen and Timokha, 2001; Wang and Khoo, 2005).

With the rapid development of computer technology, numerical model becomes more and more popular. In the early years, numerical models based on potential theory were developed by solving Laplace equation. The boundary element method was used to study sloshing (Faltinsen, 1978; Nakayama and Washizu, 1981; Iseki and Shinkai, 1988). The finite element method was also a powerful method. Nonlinear sloshing in a 2-D rectangular tank under pitch excitation was modelled and analysed (Nakayama and Washizu, 1981). The 3-D sloshing was also investigated numerically (Wu et al., 1998). A more general numerical model is to solving the Navier-Stokes equations. The finite difference method is also popular. A 3-D numerical model based on Navier–Stokes equations was proposed to simulate sloshing flows (Kim et al. 2004). A fully 3-D sloshing model based on RANS was used to study the violent sloshing (Liu and Lin, 2008).

The above works are generally focused on regular excitations. However, in general, in actual sea environment, the sea waves are not always regular, and can even be random. The behaviours of ocean structures can also be random, and the corresponding storage tanks' sloshing is also irregular or random. Forecasting the sloshing wave heights and hydrodynamic forces under sea waves are very important. A Perturbation Method of direct spectrum analysis was used to study the irregular response of the offshore platform (Zheng and Cheng, 1992). The irregular narrow-bounded wave train was

---

analytically analyzed (Petti, 1994). The 2-D sloshing under horizontal random excitations was numerically investigated by finite element method (Wang and Khoo, 2005). The sloshing under horizontal and vertical random excitations was also numerically considered (Sriram et al. 2006). However, the above works do not give wave heights which represent the real random excitations accurately, it is necessary to develop a novel method to forecast the wave height, and the corresponding hydrodynamic force can be easily deduced from the Bernoulli equation.

In the present work, a 2-D rectangular tank under random surge excitations is investigated analytically and numerically. Based on linear wave theory (Faltinsen, 1978), we deduce a more general analytic solution for tanks under random forced surge excitations. The random excitation is also obtained by linear wave theory considering a special wave spectrum with a real sea condition from the South China Sea. The analytical solutions are compared with numerical results from a two-phase fluid model, by solving the spatially averaged Navier-Stokes equations constructed on a non-inertial reference frame, and good agreements have been obtained.

## 2 Linear theory

We adopt the linear wave theory to study sloshing induced by random excitations. We just studied the 2-D tank for illustration. The tank length is  $2a$ ,  $h$  is the filling depth (mean water depth), see Figure 1. The liquid is assumed to be inviscid and irrotational. The fully nonlinear governing equations of the liquid motion can be expressed as follows (Faltinsen, 1978). There exists a velocity potential  $\phi$  satisfying the Laplace equation as Eq. [1]:

$$\frac{\partial^2 \phi}{\partial x^2} + \frac{\partial^2 \phi}{\partial z^2} = 0. \quad (1)$$

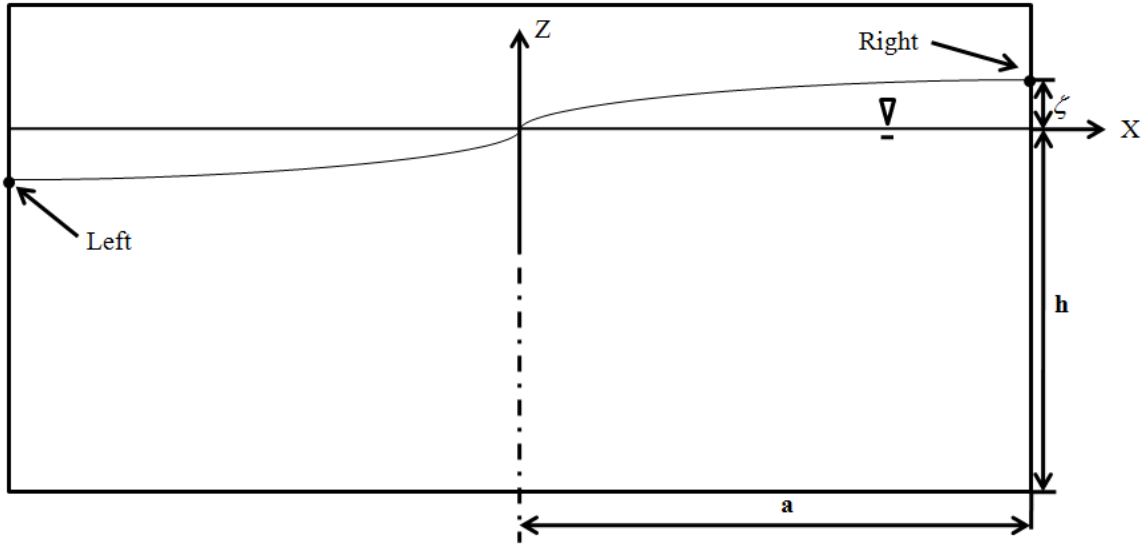


Figure 1. Schematic model of Cartesian coordinate systems.

The kinematic free-surface boundary condition can be expressed as:

$$\frac{\partial \zeta}{\partial t} = \frac{\partial \phi}{\partial z} - \frac{\partial \phi}{\partial x} \frac{\partial \zeta}{\partial x}, \quad (2)$$

where  $\zeta$  represents the free-surface elevation.

In order to model the viscous effect, Faltinsen (1978) introduced a fictitious term to the standard Euler equation as:

$$\frac{D\vec{v}}{Dt} = -\frac{1}{\rho} \nabla p - g \nabla z - \mu \nabla \phi, \quad (3)$$

where  $\vec{v}$ ,  $p$ ,  $g$  and  $\mu$  are fluid velocity, pressure, gravity and viscosity coefficient, respectively. By integration, the linearized dynamic condition on the free surface can be written as (This is just validated for the free vibration.):

$$\frac{\partial^2 \phi}{\partial t^2} + \mu \frac{\partial \phi}{\partial t} + g \frac{\partial \phi}{\partial z} = 0. \quad (4)$$

Faltinsen (1978) considered the forced surge motion, and the displacement of the tank is given by:

$$X(t) = A_1 \sin \omega t, \quad (5)$$

and the boundary condition for the fluid are:

$$\frac{\partial \phi}{\partial n} = \mp A_1 \cos \omega t \quad \text{on } x = \pm a \quad \text{and} \quad \frac{\partial \phi}{\partial n} = 0 \quad \text{on } y = -h, \quad (6)$$

where  $A_1$ ,  $\omega$  and  $\frac{\partial \phi}{\partial n}$  are oscillation amplitude, excitation angular frequency and normal derivative into the fluid, respectively.

### 3 Random wave excitation

As well known, a random wave may be generated through a specified wave spectrum, and the linear theory is usually used to simulate random sea waves, here we choose Bretschneider spectrum for illustration:

$$S_\eta(\omega) = \frac{5H_s^2}{16\omega_p} \left( \frac{\omega_p}{\omega} \right)^5 \exp \left[ -\frac{5}{4} \left( \frac{\omega_p}{\omega} \right)^4 \right], \quad (7)$$

where  $H_s$  is the significant wave height, and  $\omega_p$  is the peak frequency.

The free surface wave elevation can be obtained by linear superposition of monochromatic linear waves as

$$\eta(t) = \sum_{n=1}^{\infty} \eta_n(t) = \sum_{n=1}^{\infty} A_n \cos(\omega_n t + \varphi_n), \quad (8)$$

where  $\eta_n(t)$  is the  $n$ -th wave height,  $A_n = \sqrt{2S_\eta(\omega)\Delta\omega}$  is the  $n$ -th wave amplitude,  $t$  is time,  $\omega_n$  is the frequency of the  $n$ -th linear wave, and  $\varphi_n$  is the  $n$ -th phase of each linear wave which is uniformly distributed between 0 and  $2\pi$ , respectively.

In practice, since higher frequencies have little influence on the generated waves, we choose a certain range of frequency. Considering that a finite series of monochromatic linear waves is applicable, we set the number of summation as  $N$ , and the corresponding dispersion relationships are  $\omega_n^2 = gk_n \tanh k_n h$ , where  $h$  is the still water depth, and  $k_n$  is wave number.

From the linear wave theory, the horizontal and vertical velocities are

$$u = \sum_{n=1}^N A_n \omega_n \frac{\cosh k_n (h + \eta_n)}{\sinh k_n h} \cos(\omega_n t + \varphi_n), \quad (9)$$

and

$$w = -\sum_{n=1}^N A_n \omega_n \frac{\cosh k_n (h + \eta_n)}{\sinh k_n h} \sin(\omega_n t + \varphi_n), \quad (10)$$

and the corresponding horizontal and vertical acceleration are

$$a_x = -\sum_{n=1}^N A_n \omega_n^2 \frac{\cosh k_n (h + \eta_n)}{\sinh k_n h} \sin(\omega_n t + \varphi_n), \quad (11)$$

and

$$a_z = -\sum_{n=1}^N A_n \omega_n^2 \frac{\cosh k_n (h + \eta_n)}{\sinh k_n h} \cos(\omega_n t + \varphi_n). \quad (12)$$

In this section, we choose the real measured data to duplicate random waves, and the Fenjin FPSO, which is about 150km away to the east coastline of Hainan Island, located at Wenchang offshore oil-field, in the South China Sea is adopted. The real data can be found from that of Hu et al. (Hu et al., 2011). The water depth is 119.5m. During the typhoon *Soudelor* on July 11<sup>th</sup> in 2009, the maximal wind speed is 24.6m/s, the significant wave height is 3.1m, the mean wave period is 12.7s, and the peak period is  $T_p = 14.319s$ . All those real data are substituted into the Bretschneider spectrum to generate the real random wave, and we cut off all the frequencies beyond  $5\omega_p$ . Meanwhile, we divide the frequency domain into 500 uniform internals, which means  $N$  is 500 with corresponding  $\Delta\omega$  to be  $0.01 * \omega_p$ , which is sufficient enough to describe a random wave. The corresponding wave energy spectrum is shown in Figure 2, and the generated time curve of wave height is shown in Figure 3. In this study, we just focus on random surge excitations, and the horizontal velocity and acceleration component at the free surface are shown in Figure 4. The FFT spectral analysis of acceleration

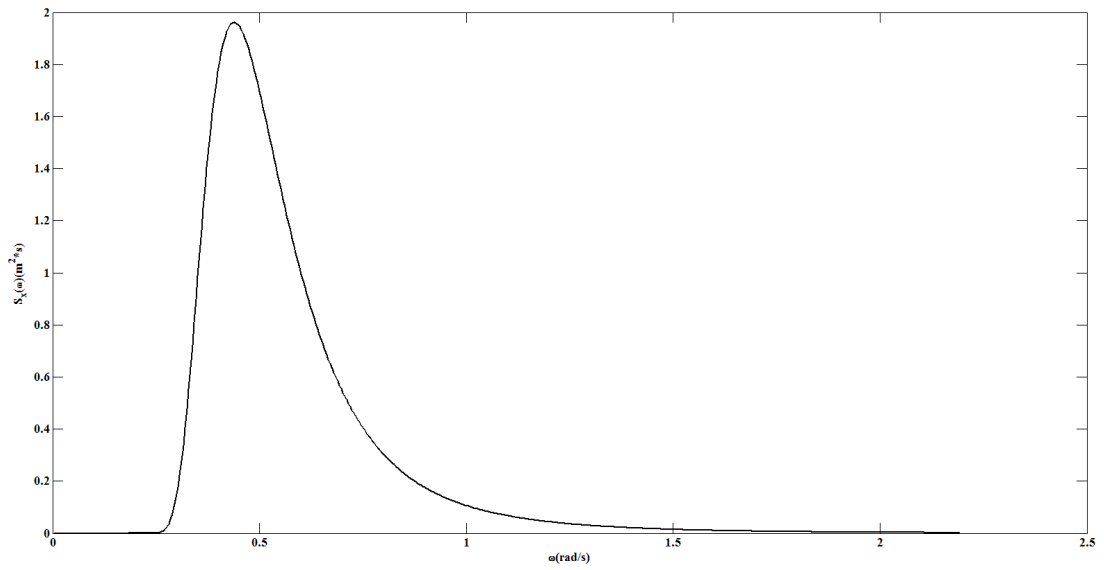


**Figure 2. Wave energy spectrum at observation spot.**

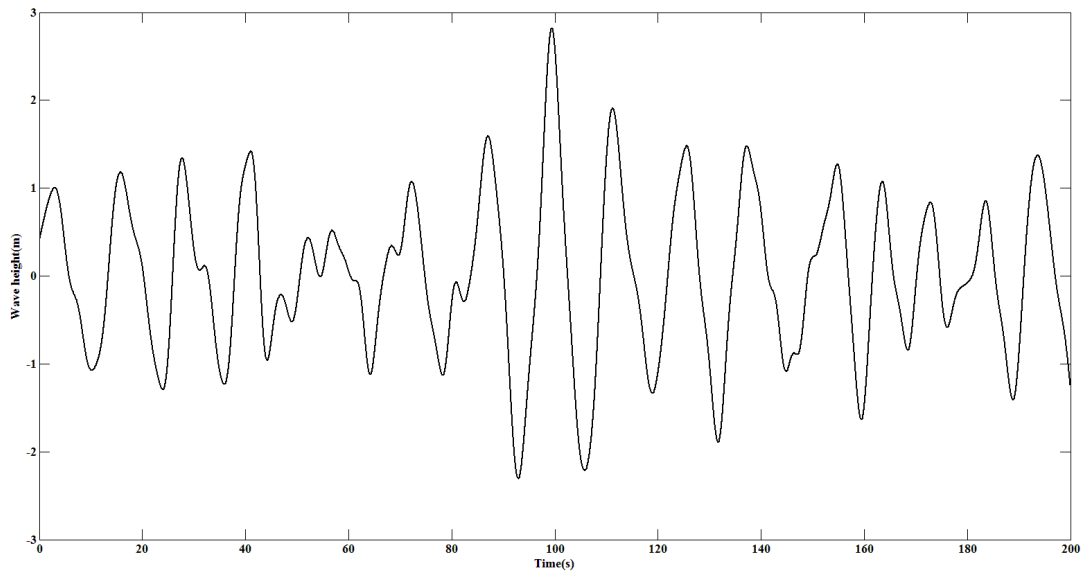


**Figure 3. Time history of free surface displacement at observation spot.**

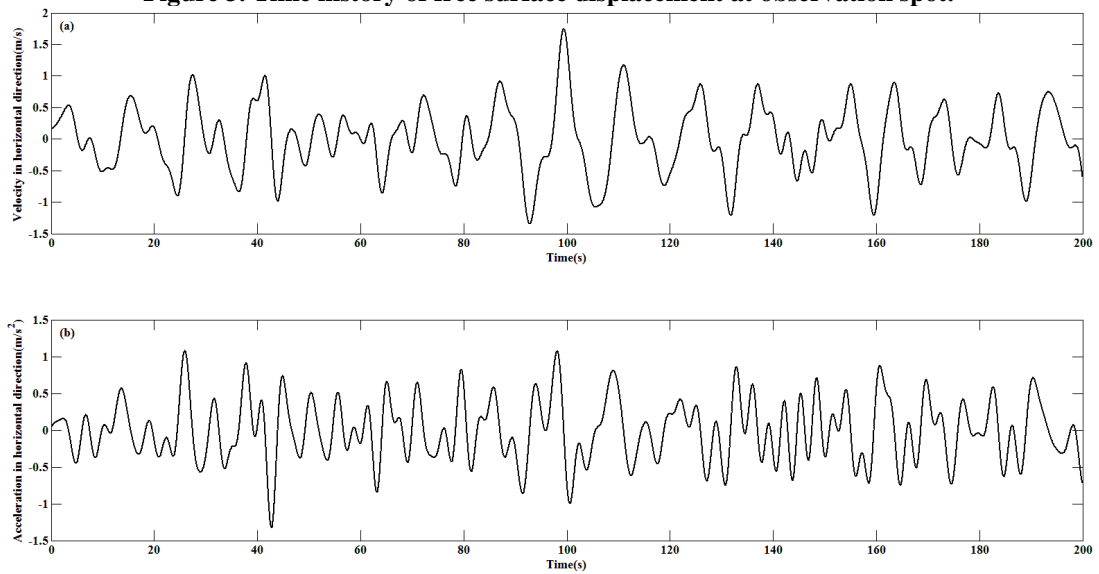


**Figure 4. Horizontal velocity (a) and particle acceleration (b) at the free surface.**

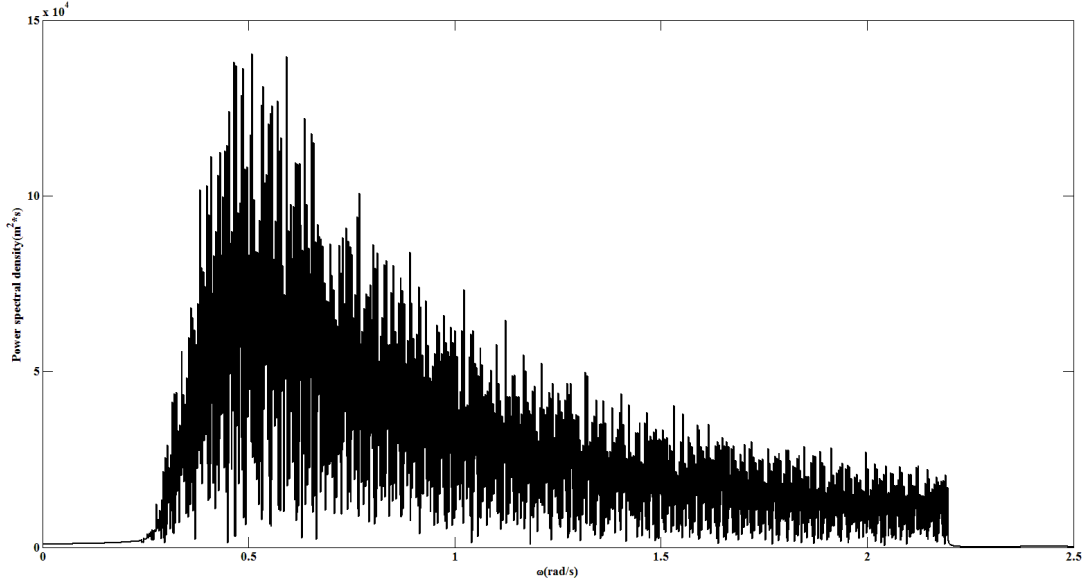


**Figure 5. FFT power spectrum of horizontal acceleration component at the free surface.**

component at free surface is shown in Figure 5. From Eq. [8] and Eq. [11], it is easy to make a conclusion that the wave spectrum and the horizontal acceleration spectrum are quite different.

#### 4 Sloshing under random surge wave excitations

In order to have a better understanding of sloshing under the real random sea state, as well as simplify the wave induced sloshing which is very complicated, we may assume that the partially filled container is excited by the water particle motion, and does not consider the counter-acting force of the sloshing to the wave motion. Under the above assumptions, by the linear wave theory, we deduce theoretical sloshing solution under real sea horizontal excitations (surge oscillation). From Eq. [11], we can draw a conclusion that the key to the analytic solution is to find the theoretical resolution of forced-surge excitation with arbitrary phase, that is, the oscillation displacement is assumed to be  $-a \sin(\omega t + \varphi)$  with  $a$  be the displacement amplitude.

##### 4.1 Analytical solution for monochromatic surge excitations

Wu et al. (1998) considered the forced wave behaviour, and explained the physical meaning of the time-dependent free-surface elevation into two terms: one corresponds to the excitation frequency with a convective velocity potential,  $\phi_C$ , the second corresponds to the natural frequencies with an impulsive velocity potential,  $\phi_I$ , and the total potential is  $\phi = \phi_C + \phi_I$ . For oscillation displacement as  $-a \sin(\omega t + \varphi)$ , the convective potential is  $\phi_C = -A \cos(\omega t + \varphi)x$ . Similar to the derivation process of Faltinsen (1978), recalling Eq. [4] and Eq. [6], it follows that

$$\frac{\partial^2 \phi_I}{\partial t^2} + \mu \frac{\partial \phi_I}{\partial t} + g \frac{\partial \phi_I}{\partial z} = -\left\{ \omega^2 A \cos(\omega t + \varphi) + \mu \omega A \sin(\omega t + \varphi) \right\} x, \quad (13)$$

with the boundary condition  $\frac{\partial \phi}{\partial n} = 0$  on  $z = -h$ .

By solving Eq. [13] and considering initial condition  $\phi$  and  $\frac{d\phi}{dt} = 0$  on the free surface, we can write the total velocity potential as:

$$\phi = \sum_{n=0}^{\infty} \sin \left\{ \frac{(2n+1)\pi}{2a} x \right\} \left\{ \begin{array}{l} -A \cos(\omega t + \varphi) \frac{2}{a} \left( \frac{2a}{(2n+1)\pi} \right)^2 (-1)^n \\ + \cosh \left( \frac{2n+1}{2a} (z+h) \right) \left[ \begin{array}{l} e^{-\frac{\mu}{2}t} (A_n \cos \sqrt{\omega_n^2 - \frac{\mu^2}{4}} t + B_n \sin \sqrt{\omega_n^2 - \frac{\mu^2}{4}} t) \\ -C_n \cos(\omega t + \varphi) - D_n \sin(\omega t + \varphi) \end{array} \right] \end{array} \right\}, \quad (14)$$

with corresponding parameters to be:

$$A_n = \frac{A \cos(\varphi)}{\cosh \left\{ \frac{(2n+1)\pi}{2a} h \right\}} \frac{2}{a} \left( \frac{2a}{(2n+1)\pi} \right)^2 (-1)^n + C_n \cos(\varphi) - D_n \sin(\varphi), \quad (15)$$

$$B_n = \frac{1}{\sqrt{\omega_n^2 - \frac{\mu^2}{4}}} \left( \frac{A \omega \sin(\varphi)}{\cosh \left\{ \frac{(2n+1)\pi}{2a} h \right\}} \frac{2}{a} \left( \frac{2a}{(2n+1)\pi} \right)^2 (-1)^n + \frac{\mu}{2} A_n \right), \quad (16)$$

$$\left. \begin{array}{l} -C_n \omega \sin(\varphi) - D_n \omega \cos(\varphi) \end{array} \right)$$

$$C_n = \frac{\omega K_n}{\omega_n^2 - \omega^2}, \quad (17)$$

$$D_n = \frac{\mu K_n (\omega_n^2 - \omega^2) + \mu \omega^2 K_n}{(\omega_n^2 - \omega^2)^2 + \mu^2 \omega^2}. \quad (18)$$

The final free surface elevation can be written as

$$\eta = \frac{1}{g} \sum_{n=0}^{\infty} \sin \left\{ \frac{(2n+1)\pi}{2a} x \right\} \left\{ \begin{array}{l} -A \omega \sin(\omega t + \varphi) \frac{2}{a} \left( \frac{2a}{(2n+1)\pi} \right)^2 (-1)^n \\ + \cosh \left\{ \frac{(2n+1)\pi}{2a} h \right\} * \left\{ \begin{array}{l} -\frac{\mu}{2} e^{-\frac{\mu}{2}t} \left( A_n \cos \sqrt{\omega_n^2 - \frac{\mu^2}{4}} t + B_n \sin \sqrt{\omega_n^2 - \frac{\mu^2}{4}} t \right) \\ + e^{-\frac{\mu}{2}t} \left( -A_n \sqrt{\omega_n^2 - \frac{\mu^2}{4}} \sin \sqrt{\omega_n^2 - \frac{\mu^2}{4}} t + B_n \sqrt{\omega_n^2 - \frac{\mu^2}{4}} \cos \sqrt{\omega_n^2 - \frac{\mu^2}{4}} t \right) \\ - C_n \omega \sin(\omega t + \varphi) + D_n \omega \cos(\omega t + \varphi) \end{array} \right\} \end{array} \right\}. \quad (19)$$

## 4.2 Liquid sloshing under surge excitation with arbitrary phases

The theoretical solution is compared with the numerical result obtained from the numerical model derived by Liu and Lin (2007). Here we will introduce it in brief, and more details can be found in Liu and Lin (2007). It is a two-phase fluid model, by solving the spatially averaged Navier-Stokes equations constructed on a non-inertial reference frame with six degree-of-freedom (DOF) of motions. The two-step projection method is adopted in the numerical simulation, and the Bi-CGSTAB technique is applied to solve the pressure Poisson equation. The second-order Yong's volume-of-fluid (VOF) method is used to track the free surface. In verifying the analytical solution, we consider the case  $\mu = 0$ , and neglect the viscous effect.

Here we consider a tank with dimensions  $0.57m \times 0.30m$ , and the still water depth  $0.15m$ , thus the lowest natural frequency is  $\omega_0 = 6.0579 \text{ rad/s}$ , and  $\omega$  is the angular frequency of the external excitation. Three different frequencies  $6.0579 * 0.2 \text{ rad/s}$ ,  $6.0579 * 0.7 \text{ rad/s}$  and  $6.0579 * 0.9 \text{ rad/s}$  are simulated with the same acceleration amplitude

$0.002m/s^2$ . Three different phases  $\frac{\pi}{4}$ ,  $\frac{3\pi}{4}$  and  $\frac{3\pi}{2}$  are also considered.

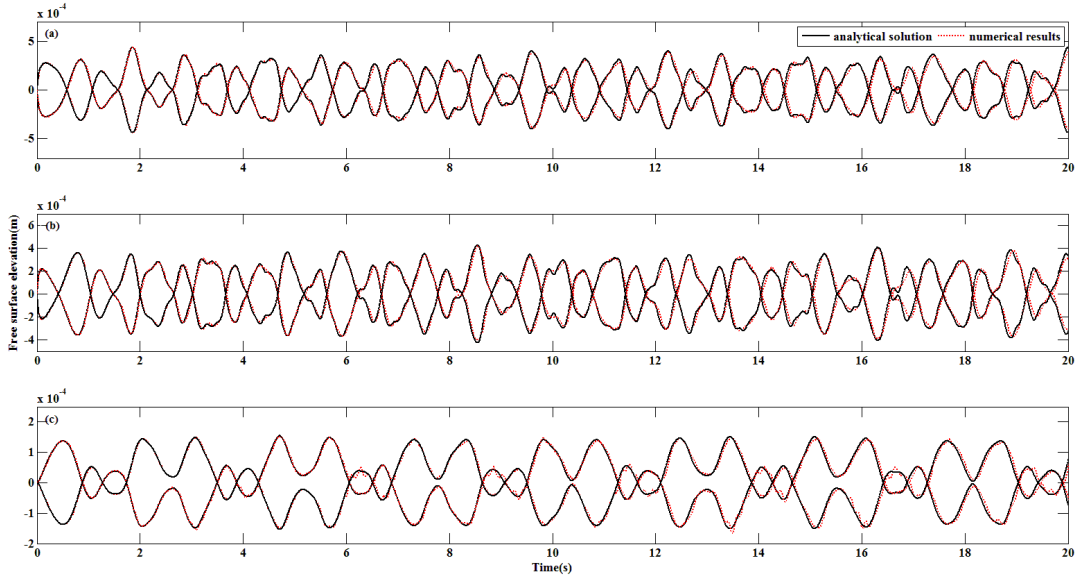


**Figure6. Comparisons of free surface displacement at  $x = \pm 0.285m$  with (a)  $\varphi = \frac{\pi}{4}$ ; (b)  $\varphi = \frac{3\pi}{4}$ ; (c)  $\varphi = \frac{3\pi}{2}$  between the numerical results (dotted line) and analytical solution (solid line).**

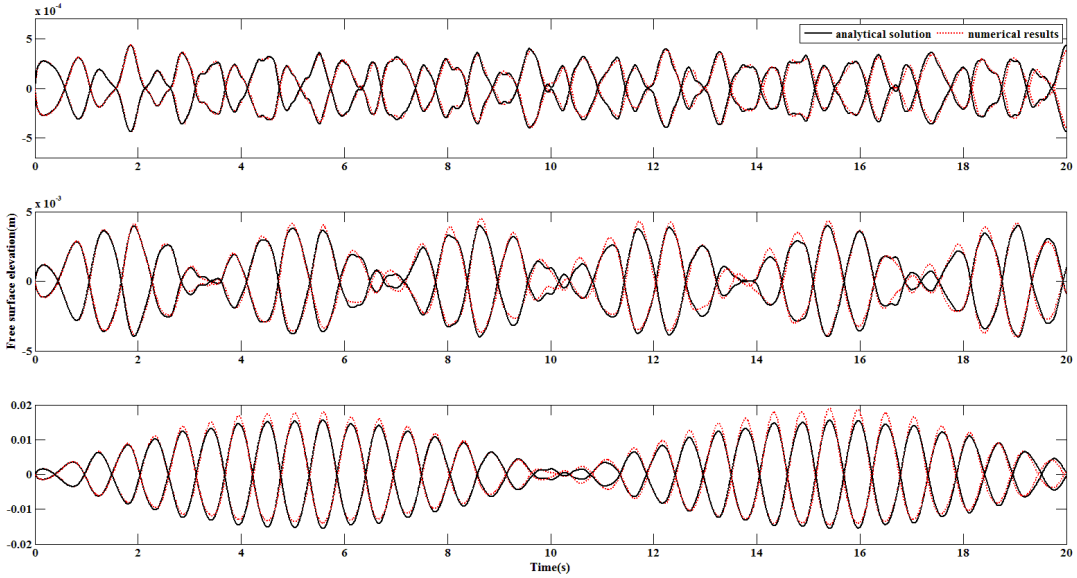


**Figure7. Comparisons of free surface displacement at  $x = \pm 0.285m$  with (a)  $\omega = 6.0579 * 0.2 \text{ rad/s}$ ; (b)  $\omega = 6.0579 * 0.7 \text{ rad/s}$ ; (c)  $\omega = 6.0579 * 0.9 \text{ rad/s}$  between the numerical results (dotted line) and analytical solution (solid line).**

In the numerical simulation, we employ 114 uniform horizontal meshes and 100 uniform vertical meshes. The time step is automatically adjusted to ensure the numerical stability. With the fixed natural frequency  $6.0579 * 0.2 \text{ rad/s}$ , three different phases  $\frac{\pi}{4}$ ,  $\frac{3\pi}{4}$  and  $\frac{3\pi}{2}$  are simulated. The numerical results of the free surface at  $x = \pm 0.285m$  are compared with the analytical solution Eq. (16) in Figure 6. Good agreements have been obtained, and the analytical solution is verified. Meanwhile, with the fixed phase  $\frac{\pi}{4}$ , three different frequencies are also considered, that is  $6.0579 * 0.2 \text{ rad/s}$ ,  $6.0579 * 0.7 \text{ rad/s}$  and  $6.0579 * 0.9 \text{ rad/s}$ . The numerical results of free surface at  $x = \pm 0.285m$  are also compared with the analytical solution Eq. (16) in Figure 7. With the frequency increasing close to the lowest natural frequency, the discrepancy becomes more and more obvious, and this is mainly due to the fact that the non-linear effect becomes

non-negligible which can be verified from Figure 7(b) and Figure 7(c)—a typical non-linear phenomenon with sharper crest and flatter trough.

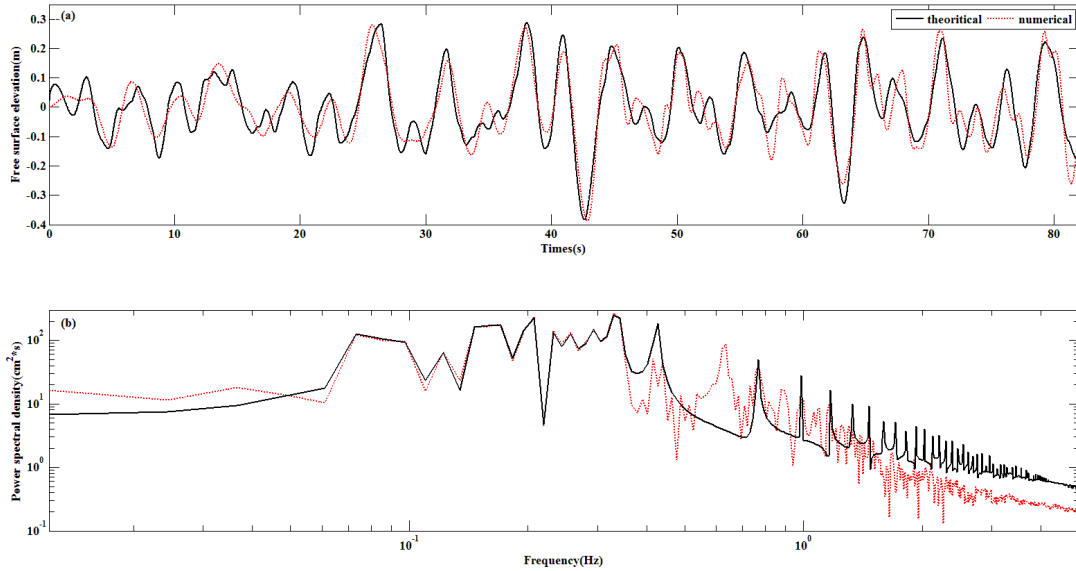


**Figure8.** Comparisons of free surface displacement and corresponding power spectrum at  $x = \pm 2.0$  between the numerical result (dotted line) and analytical solution (solid line).

### 4.3 Liquid sloshing under random wave excitations

In this section, the sloshing under forced random surge motions is analytically analysed. The length of the sloshing tank is  $4.0m$ , and the water depth is  $2.0m$ , thus the lowest natural frequency is  $\omega_0 = 2.6583 \text{ rad/s}$ . The tank is subjected to forced surge excitation as shown in Figure 4 (b). Though this study, all the results are derived from the linear wave theory, thus, similar to the generation of the random or irregular waves, the wave heights under random surge oscillations can also be written as the summation of each wave height of single oscillation. As shown in Section 3, we have decomposed the random excitation into 500 different components, meanwhile, the analytical solution of each component has been derived in Section 4.1 and verified in Section 4.2. The free surface elevations of the left corner and the corresponding FFT spectral analysis are shown in Figure 8. The discrepancy of free surface elevations between the analytical and numerical results is obvious in the first few seconds, and decreases gradually. This is mainly due to the relatively non-zero strong initial acceleration's perturbation. The phase difference between the analytical and numerical solution is small. Furthermore, the analytical free surface elevation agrees well with the numerical result, and the difference may mainly due to the analytical solution consider the linearized free-surface boundary condition. In a word, the difference between the numerical result and analytical solution is acceptable, the analytical solution can forecast the wave height to some extent, and is applicable in the practical engineering. Furthermore, from the solid line of Figure 8(b), we find that the second peak is about  $0.4269 \text{ Hz}$  which is close to the lowest natural frequency  $\omega_0$  ( $0.4231 \text{ Hz}$ ). From Figure 5, the cut-off frequency is about  $2.5 \text{ rad/s}$ , which is also below the lowest natural frequency, that is, all the excitations are less than the resonant frequency. If the simulation time is long enough, the first peak region should be occurred near  $0.06 \text{ Hz}$ , which is close to the peak of FFT power acceleration spectrum, see Figure 5.

## 5 Conclusion

An analytical solution is derived for forced surge oscillation with arbitrary phases. A series of numerical tests have conducted to estimate the analytical solution. Very good agreements of free surface elevations have been obtained except for the oscillation frequency close to the lowest natural frequency. The analytical solution for random excitation has also been introduced by linear combination of all single excitations. Although there exist some discrepancies between the numerical and analytical results, the analytical solution is acceptable and can forecast the time series of free surface elevation to a certain extent, and the analytical solution can guide the design of FPSOs.

## ACKNOWLEDGEMENT

The research was supported by research grants from National Key Basic Research Program of China (2013CB036401); National Nature Science Foundation of China (51479126).

## REFERENCES

- Abramson, H.N., 1966, The dynamic behaviour of liquid in moving containers, Reports SP 106 of NASA.
- Chen, B.F., Chiang, H.W., 2000, Complete two-dimensional analysis of sea-wave- induced fully non-linear sloshing fluid in a rigid floating tank, *Journal of Ocean Engineering*, 27:953–77.
- Faltinsen, O.M., 1974, A non-linear theory of sloshing in rectangular tanks, *Journal of Ship Research*, 18(4):224–41.
- Faltinsen, O.M., 1978, A numerical non-linear method of sloshing in tanks with two-dimensional flow, *Journal of Ship Research*, 22(3):193–202.
- Faltinsen, O.M., Timokha, A., 2002, Asymptotic modal approximation of nonlinear resonant sloshing in a rectangular tank with small fluid depth, *Journal of Fluid Mechanics*, 470:319–57.
- Hu, Z.Q., Yang, J.M., Zhao, Y.N., Bai, G., 2011, Full scale measurement for FPSO on motions in six-degrees of freedom and environmental loads and deduction of mooring system loads, *SCIENCE CHINA(Physics, Mechanics & Astronomy)*, 54(1): 26–34.
- Ibrahim, R.A., Pilipchuk, V.N., Ikeda, T., 2001, Recent advances in liquid sloshing dynamics, *Appl. Mech. Rev.* 54: 133–199.
- Iseki, T., Shinkai, A., 1988, Boundary element analysis of non-linear sloshing problems using cubic element, *Journal of the Society of Naval Architects of Japan*, 163:294–301.
- Kim, Y., Shin, Y.S., Lee, K.H., 2004, Numerical study on slosh-induced impact pressures on three-dimensional prismatic tanks, *Appl Ocean Res*, 26:213–226.
- Liu, D.M., Lin, P.Z., 2008, A numerical study of three dimensional liquid sloshing in tanks, *Journal of Computational Physics*, 227:3921–3939.
- Nakayama, T., Washizu, K., 1980, Nonlinear analysis of liquid motion in a container subjected to forced pitching oscillation, *Int. J. Numer. Method Eng.* 15:1207–1220.
- Nakayama, T., Washizu, K., 1981, The boundary element method applied to the analysis of two-dimensional nonlinear sloshing problems. *International Journal for Numerical Methods in Engineerings*, 17: 631–1646.
- Petti, M., 1994. Third-order analysis of nonlinearities bounded to narrow banded spectra, *International Journal of Offshore and Polar Engineering*, 4:257–264.
- Sriram, V., Sannasiraj, S.A., Sundar, V., Numerical simulation of 2D sloshing waves due to horizontal and vertical random excitation, *Applied Ocean Research*, 28:19–32.
- Van der Vorst, H.A., 2003, *Iterative Krylov Methods for Large Linear Systems*, Cambridge University Press, New York, USA.
- Wang, C.Z., Khoo, B.C., 2005, Finite element analysis of two-dimensional nonlinear sloshing problems in random excitation, *Ocean Engineering*, 32:107–133.
- Wang, C.Z., Khoo, B.V., 2005, Finite element analysis of two-dimensional nonlinear sloshing problems in random excitations, *Ocean Engineering*, 32:107–133.
- Wu, G.X., Ma, Q.W., Eatock Taylor, R., 1998. Numerical simulation of sloshing waves in a 3D tank based on a finite element method. *Applied Ocean Research*, 20:337–355.
- Zheng, Z.C., Cheng, B.R., 1992. A perturbation method of direct spectral analysis for the random response of offshore structures, *International Journal of Offshore and Polar Engineering*, 2:7–12.
-